THE FASEB JOURNAL • RESEARCH • www.fasebj.org

Tackling MARCKS-PIP3 circuit attenuates fibroblast activation and fibrosis progression

David C. Yang,[*,†,‡] Ji-Min Li,[‡] Jihao Xu,[‡] Justin Oldham,[*,†] Sem H. Phan,[§] Jerold A. Last,[*,†] Reen Wu,[*,†] and Ching-Hsien Chen[‡,1]

[*]Division of Pulmonary and Critical Care Medicine and [‡]Division of Nephrology, Department of Internal Medicine, and [†]Department of Internal Medicine, Center for Comparative Respiratory Biology and Medicine, University of California–Davis, Davis, California, USA; and [§]Department of Pathology, University of Michigan School of Medicine, Ann Arbor, Michigan, USA

ABSTRACT: Targeting activated fibroblasts, including myofibroblast differentiation, has emerged as a key therapeutic strategy in patients with idiopathic pulmonary fibrosis (IPF). However, there is no available therapy capable of selectively eradicating myofibroblasts or limiting their genesis. Through an integrative analysis of the regulator genes that are responsible for the activation of IPF fibroblasts, we noticed the phosphatidylinositol 4,5-bisphosphate (PIP2)-binding protein, myristoylated alanine-rich C-kinase substrate (MARCKS), as a potential target molecule for IPF. Herein, we have employed a 25-mer novel peptide, MARCKS phosphorylation site domain sequence (MPS), to determine if MARCKS inhibition reduces pulmonary fibrosis through the inactivation of PI3K/protein kinase B (AKT) signaling in fibroblast cells. We first observed that higher levels of MARCKS phosphorylation and the myofibroblast marker α-smooth muscle actin (α-SMA) were notably overexpressed in all tested IPF lung tissues and fibroblast cells. Treatment with the MPS peptide suppressed levels of MARCKS phosphorylation in primary IPF fibroblasts. A kinetic assay confirmed that this peptide binds to phospholipids, particularly PIP2, with a dissociation constant of 17.64 nM. As expected, a decrease of phosphatidylinositol (3,4,5)-trisphosphate pools and AKT activity occurred in MPS-treated IPF fibroblast cells. MPS peptide was demonstrated to impair cell proliferation, invasion, and migration in multiple IPF fibroblast cells *in vitro* as well as to reduce pulmonary fibrosis in bleomycin-treated mice *in vivo*. Surprisingly, we found that MPS peptide decreases α-SMA expression and synergistically interacts with nintedanib treatment in IPF fibroblasts. Our data suggest MARCKS as a druggable target in pulmonary fibrosis and also provide a promising antifibrotic agent that may lead to effective IPF treatments.—Yang, D. C., Li, J.-M., Xu, J., Oldham, J., Phan, S. H., Last, J. A., Wu, R., Chen, C.-H. Tackling MARCKS-PIP3 circuit attenuates fibroblast activation and fibrosis progression. FASEB J. 33, 14354–14369 (2019). www.fasebj.org

KEY WORDS: pulmonary fibrosis · drug efficacy · AKT signaling · nintedanib · phospholipids

Idiopathic pulmonary fibrosis (IPF) is a progressive interstitial lung disease with poor prognosis and a median survival of 2–3 yr. Of great concern, there are no currently available therapies to stop disease progression (1, 2). Although there are 2 therapeutic drugs presently in clinical use—nintedanib and pirfenidone—adverse effects due to treatment sometimes necessitated dose reduction and/or treatment interruption (3–5). Pirfenidone is an anti-inflammatory and antifibrotic drug widely used for IPF that has been shown to affect TGF-β–mediated fibroblast activity; unfortunately, its mechanism of action is poorly defined. Treatment with pirfenidone often results in adverse effects such as photosensitivity, gastrointestinal problems, skin rashes, and more, sometimes necessitating dose reduction (6). Nintedanib, an intracellular multikinase inhibitor, in particular shows antifibrotic and anti-inflammatory effects *via* blocking several key receptor tyrosine kinases, including platelet-derived growth factor receptor (PDGFR), fibroblast growth factor receptor (FGFR), and VEGF receptor (VEGFR) (7, 8). However, this drug does not completely inhibit the TGF-β pathway, an important determinant in IPF pathogenesis (9, 10). Furthermore, adverse effects are common with nintedanib

ABBREVIATIONS: α-SMA, α–smooth muscle actin; AKT, protein kinase B; CI, combination index; COL1A1, collagen, type I, α-I chain; dd, double distilled; ECM, extracellular matrix; FGFR, fibroblast growth factor receptor; FN1, fibronectin 1; IHC, immunohistochemical; IPF, idiopathic pulmonary fibrosis; MARCKS, myristoylated alanine-rich C-kinase substrate; MPC, MARCKS phosphorylation site domain sequence; PDGFR, platelet-derived growth factor receptor; PIP2, phosphatidylinositol 4,5-bisphosphate; PIP3, phosphatidylinositol (3,4,5)-trisphosphate; PSD, phosphorylation site domain; shRNA, short hairpin RNA; TBP, TATA-binding protein; VEGFR, VEGF receptor

[1] Correspondence: Division of Nephrology, Department of Internal Medicine, University of California Davis, 451 East Health Sciences Dr., GBSF 6311, Davis, CA 95616, USA. E-mail: jchchen@ucdavis.edu

doi: 10.1096/fj.201901705R

This article includes supplemental data. Please visit *http://www.fasebj.org* to obtain this information.

0892-6638/19/0033-14354 © FASEB

therapy and worsen with higher dosages, which result in drug discontinuation (11–13). Steroid therapy with corticosteroids, along with other inflammatory drugs, had long been standard therapy for patients with IPF worldwide. However, the lack of large randomized controlled monotherapy trials, minor benefit of treatment, and significant morbidity from long-term corticosteroid treatments have resulted in recommendations against use since 2011 and 2015 (14, 15). Because of a lack of efficacy, unclear mechanisms of action, and unfavorable adverse effect profiles of current therapies, there is an urgent need to seek new and improved therapeutics for those diagnosed with IPF.

Fibroblasts, specifically myofibroblasts, have been implicated to play a major role in the progression of IPF through formation of fibroblastic foci, excessive deposition of extracellular matrix (ECM), alveolar architecture distortion, and collagen deposition (16, 17). Under normal conditions, fibroblasts express little ECM production and cell-to-cell actin contacts. However, after initial injury, fibroblasts can differentiate into myofibroblasts, a contractile and secretory phenotype marked by expression of α–smooth muscle actin (α-SMA), which is indicative of fibroblast activation and plays a critical role in the development and progression of IPF (18, 19). This activated phenotype can impair lung function through tissue contraction and excessive deposition of ECM. Previous studies have demonstrated that multiple signaling proteins, such as TGF-β, PI3K, and protein kinase B (AKT), are involved in influencing fibroblast activation, myofibroblast differentiation, and survival contributing to disease progression (9, 10, 20–22). Specifically, the transcription factor AKT has been identified as a major convergence factor of PDGFR and TGF-β signaling in IPF progression. Upon activation, TGF-β is a potent growth factor and can induce both the PDGFR and PI3K/AKT pathways, subsequently promoting fibroblast recruitment, myofibroblast survival, and proliferation (22, 23). These long-lived myofibroblasts play a major role in fibrosis, but the detailed molecular mechanisms underlying fibroproliferative disorders is still incompletely understood.

Through an integrative analysis of the regulator genes that are responsible for the activation of IPF fibroblasts, we noticed the dysregulation of myristoylated alanine-rich C-kinase substrate (MARCKS), a major PKC substrate. MARCKS, a phospholipid binding protein, is a key regulatory protein controlling cell migration, exocytosis, and phagocytosis (24–26). Recent studies have indicated that an important function of the MARCKS phosphorylation site domain (PSD), upon phosphorylation, is to provide PI3K with phosphatidylinositol 4,5-bisphosphate (PIP2) pools for phosphatidylinositol (3–5)-trisphosphate (PIP3) production, thereby activating AKT (27–29). Based on the sequence of the MARCKS PSD, we previously identified a 25-mer peptide, the MPS peptide, which targets the MARCKS PSD sequence (MPS) and inhibits AKT activation in cancers (28, 30).

In this study, we show that phosphorylated MARCKS is up-regulated in IPF tissues and in a mouse pulmonary fibrosis model. In addressing the lack of an effective treatment for IPF, we have not only identified the 25-mer peptide MPS as a novel fibrotic agent but also provided an alternative therapeutic strategy of improving the efficacy of the multikinase inhibitor nintedanib for IPF treatment.

MATERIALS AND METHODS

Materials

DMEM, Roswell Park Memorial Institute (RPMI)1640 medium, fetal bovine serum, and penicillin-streptomycin were purchased from Thermo Fisher Scientific (Waltham, MA, USA). Lipofectamine and anti-PIP3 antibody were also purchased from Thermo Fisher Scientific). Vectastain Elite ABC Kit (rabbit IgG), Vector Hematoxylin QS nuclear counterstain, and 3,3′-diaminobenzidine (DAB) solution were purchased from Vector Laboratories (Burlingame, CA, USA). Anti-phosphorylated (p)Ser158 MARCKS (clone EP2113Y) and anti-MARCKS (clone EP1446Y) were purchased from Abcam (Cambridge, MA, USA). Anti-pSer159/163 MARCKS (clone D13D2), anti-pSer473 AKT, anti-pSer308 AKT, anti-AKT, anti–α-SMA, anti–glyceraldehyde 3-phosphate dehydrogenase, and anti–β-actin antibodies were purchased from Cell Signaling Technology (Danvers, MA, USA). Hydroxyproline assay kits were purchased from MilliporeSigma (Burlington, MA, USA).

Plasmid constructs and primers

For generation of MARCKS short hairpin RNA (shRNA) plasmids, the oligonucleotide of shRNAs (shRNA: 5′-GAGCGCTTCTCCTTCAAGAA-3′ and its complementary strand: 5′-TTCTTGAAGGAGAAGCGCTC-3′) were synthesized, annealed, and cloned into the pGreenPuro shRNA expression lentivector (System Biosciences, Palo Alto, CA, USA). All primers for real-time quantitative PCR used were as follows: the α-SMA forward, 5′-TCCTCATCCTCCCTTGAGAA-3′ and the reverse, 5′-ATGAAGGATGGCTGGAACAG-3′; the collagen, type I, α-I chain (COL1A1) forward, 5′-ACGAAGACATCCCACCAATCACCT-3′ and the reverse, 5′-AGATCACGTCATCGCACAACACCT-3′; the Thy-1 cell surface antigen (THY1) forward, 5′-AGAGACTTGGATGAGGAG-3′ and the reverse, 5′-CTGAGAATGCTGGAGATG-3′; the fibronectin 1 (FN1) forward, 5′-TCCACAAGCGTCATGAAGAG-3′ and the reverse, 5′-CTCTGAATCCTGGCATTGGT-3′; the vimentin (VIM) forward, 5′-AACTTCTCAGCATCACGATGAC-3′ and the reverse, 5′-TTGTAGGAGTGTCGGTTGTTAAG-3′; the MARCKS forward, 5′-TTGTTGAAGAAGCCAGCATGGGTG-3′ and the reverse, 5′-TTACCTTCACGTGGCCATTCTCCT-3′.

Cell culture

Human primary fibroblast cells were obtained from airway tissues provided from the University of California (UC) Davis Medical Hospital (Sacramento, CA, USA) with consent. The protocol for human tissue procurement and usage was periodically reviewed and approved by the University Human Subject Research Review Committee. Primary fibroblast cell lines, IPF-1, -2, -3, and -4 cells, were established from patients with IPF. Cells were obtained from lung biopsies, and the diagnosis of IPF was supported by patient history, physical examination, pulmonary function tests, and typical high-resolution chest computed tomography findings of IPF. In all cases, the diagnosis of IPF was confirmed by microscopic analysis of lung tissue and demonstrated the characteristic morphologic findings of usual interstitial pneumonia. All patients fulfilled the criteria for the diagnosis of IPF as established by the American Thoracic Society

and European Respiratory Society. Nonfibrotic primary control adult human lung fibroblast lines Normal-1, -2, and -3 cells were used. These lines were established from normal lung tissue or histologically normal lung tissue adjacent to carcinoid tumor. The IPF cell line, LL97A, was purchased from the American Type Culture Collection (Manassas, VA, USA). Lung fibroblast lines were cultured in high-glucose DMEM or Roswell Park Memorial Institute-1640 medium with 10% fetal bovine serum and 1% penicillin-streptomycin at 37°C in a humidified atmosphere of 5% CO_2. Fibroblasts were used less than passages 8. Cells were characterized as fibroblasts as previously described (31).

Real-time quantitative PCR

The mRNA expression level of target genes was detected by real-time RT-PCR using primers as described in the Supplemental Data. The housekeeping gene TATA-box binding protein (TBP) was used as the reference gene. The relative expression level of target genes compared with that of TBP was defined as $-\Delta C_t = -[C_{t\ \text{target}} - C_{t\ \text{TBP}}]$. The target/TBP mRNA ratio was calculated as $2^{-\Delta C_t} \times K$, where K is a constant.

Patient lung specimens and immunohistochemical staining

IPF lung tissue and non-IPF normal lung specimens were obtained from patients with histologically confirmed IPF who underwent surgical resection at the UC Davis Medical Center. This investigation was approved by the Institutional Review Board of the UC Davis Health System. Written informed consent was obtained from all patients. All patient samples were de-identified and provided by the UC Davis Interstitial Lung Disease Program. Formalin-fixed and paraffin-embedded specimens were used, and level of phospho-MARCKS was analyzed by immunohistochemical (IHC) staining as previously described (28). Detailed experimental procedures were modified from the paraffin immunohistochemistry protocol supplied by the manufacturer (Cell Signaling Technology). The slides were deparaffinized in xylene substitute and rehydrated in graded alcohol and water. An antigen retrieval step [10 nM sodium citrate (pH 6.0) at a subboiling temperature] was used for each primary antibody. Endogenous peroxidase activity was blocked by 3% hydrogen peroxide followed by blocking serum and incubation with appropriate antibodies overnight at 4°C. Detection of immunostaining was carried out by using the Vectastain ABC system, according to the manufacturer's instructions (Vector Laboratories). A 4-point staining intensity scoring system was devised to confirm the relative expression of phospho-MARCKS in lung specimens; scores ranged from 0 (no expression) to 3 (highest-intensity staining) as previously described (28, 32–34). The results were classified into 2 groups according to the intensity and extent of staining: in the low-expression group, staining was observed in 0–1% of the cells (staining intensity score = 0), in <10% of the cells (staining intensity score = 1), or in 10–25% of the cells (staining intensity score = 2); in the high-expression group, staining was present more than 25% of the cells (staining intensity score = 3).

Peptide synthesis

The MPS, control, and scrambled peptides (95% pure) were purchased from EZBiolab (Carmel, IN, USA). The MPS peptide consisted of 151–175 aa from the wild-type protein, KKKKKRFSFKKSFKLSGFSFKKNKK; the control peptide had a sequence KKKKKRFDFKKDFKLDGFDFKKNKK, and the scrambled peptide had a sequence KRFLSKKKNKSFFGKSKKFKKKKSF. Peptides were reconstituted in PBS, yielding stock concentrations of 10 mM. Stock solutions were stored at −20°C and diluted to desired concentrations on the day of the experiment.

Kinetic assay

Real-time binding of the peptide mimicking the phosphorylation site domain of MARCKS (MPS peptide, 151–175 aa from the wild-type MARCKS protein) to biotin-labeled PIP2 was evaluated using biolayer interferometry on an Octet RED96 system (FortéBio, Fremont, CA, USA) following the manufacturer's instructions. Briefly, the ligand, PIP2 labeled with biotin at the sn-1 position [1000 nM in double distilled (dd)H_2O], was immobilized on Super Streptavidin biosensors for 10 min. A binding assay was performed with the MPS analyte at various concentrations from 0 to 1000 nM in ddH_2O. Association and dissociation were monitored for 5 min. Assays were performed at 24°C. Data were analyzed using Octet Data Analysis Software 7.0 (FortéBio).

PIP3 quantitation

Cells were harvested and precipitated by trichloroacetic acid. PIP3 lipids were extracted twice from the trichloroacetic acid precipitated fraction by methanol:chloroform (2:1). After acidification, organic-phase lipids were used for PIP3 quantitation, based on the protocol for the PIP3 Mass ELISA Kit (Echelon Biosciences, Salt Lake City, UT, USA). Briefly, the lipid extract from cultured cells was mixed with the PIP3-specific detector protein, which was then incubated in a PIP3-coated microplate for competitive binding. After several washes, the microplate was then incubated with an horseradish peroxidsase–linked secondary detector and tetramethylbenzidine substrate for color development. To stop further color development, 2 M H_2SO_4 solution was then added. Microplates were read at an absorbance wavelength of 450 nm. A series of different dilutions of PIP3 standards were used to establish a standard curve for each reaction. Cellular PIP3 amounts could be estimated by comparing the absorbance in the wells with the values in the standard curve. Experiments were conducted in triplicate dishes and repeated in 2 independent cultures with cell density 5×10^6 cells/100-mm dish.

Transwell invasion assay

An *in vitro* cell invasion assay was performed as previously described (27, 28) using Transwell chambers (8-μm pore size; Costar; MilliporeSigma). Briefly, 2×10^4 cells were seeded on top of the polycarbonate filters that were coated with Matrigel (Becton Dickinson, Franklin Lakes, NJ, USA), and 0.5 ml of growth medium with scrambled or MPS peptide (100 μM) was added to both the upper and lower wells. After incubation for 20 h, filters were swabbed with a cotton swab, fixed with methanol, and then stained with Giemsa solution (MilliporeSigma). The cells attached to the lower surface of the filter were counted under a light microscope (×10 magnification).

Scratch wound healing assay

Cells were seeded to 6-well tissue culture dishes and grown to confluence. A linear wound was introduced to each confluent monolayer using a pipette tip and washed 3 times with PBS. Thereafter, cell morphology and migration were observed and photographed at regular intervals for 12 and 24 h. The number of cells migrating into the cell-free zone was acquired under a light microscope and counted.

Immunoblotting and immunofluorescent staining

Western blot analyses and the preparations of whole-cell lysates have been previously described (28, 30, 34). For whole-cell lysates, cells were lysed in a lysis buffer [50 mM Tris-HCl (pH 7.4), 1% Triton X-100, 10% glycerol, 150 mM NaCl, 1 mM EDTA, 20 μg/ml leupeptin, 1 mM PMSF, and 20 μg/ml aprotinin] and separated by SDS-PAGE. Immunoblotting was conducted using appropriate antibodies followed by chemiluminescent detection. For immunofluorescent staining, after an antigen retrieval step, tissue slides were reacted with antibodies against FITC-labeled antibody (anti-PIP3 or anti–α-SMA) and tetramethylrhodamine-conjugated antibody (anti-MARCKS or anti–phospho-MARCKS), and nuclei were demarcated with DAPI staining. The cells were mounted onto slides and visualized using fluorescence microscopy (model Axiovert 100; Carl Zeiss GmbH, Oberkochen, Germany) or a Zeiss LSM510 laser-scanning confocal microscope image system.

Bleomycin-induced lung fibrosis

Female C57BL/6J mice (8-wk-old) purchased from The Jackson Laboratory (Bar Harbor, ME, USA) were housed 4 mice/cage and fed autoclaved food *ad libitum*. These mice received saline or bleomycin intratracheally as previously described (35). Briefly, mice were anesthetized with 5% isoflurane and administered bleomycin (APP Pharmaceuticals, Schaumburg, IL, USA) at a dose of 0.005 U/g mouse *via* intratracheal aspiration on d 0. Control animals received an equal volume of sterile saline only. In early fibrogenic phase, these mice were intraperitoneally injected with either PBS, or MPS peptide (28 mg/kg) every 2 d. At 21 d of bleomycin insult, these mice were euthanized, and the lungs were collected for histologic analysis. Mouse experiments were approved by the Institutional Animal Care and Use Committee (IACUC) of University of California–Davis (UC Davis). If the event of any unexpected adverse effects arises, Campus Veterinary Services will be contacted and UC Davis IACUC policy on Humane Endpoints will be followed.

Hydroxyproline assays

Lung tissues collected from mouse experiments were cut into smaller pieces and homogenized in 100 μl ddH_2O/10 mg tissue using a sonicator (VC50 Vibra-Cell; Sonics and Materials, Newtown, CT, USA). Hydrochloric acid 100 μl (12 M)/10 mg tissue was added and samples were transferred into glass Wheaton ampules (Wheaton, Millville, NJ, USA) and sealed. Samples were hydrolyzed for 3 h at 120°C. Samples were allowed to cool, transferred into microcentrifuge tubes, and then centrifuged at 10,000 *g* for 3 min. Supernatant was retrieved and 10–50 μl were transferred to a clear 96-well flat-bottomed plate. The plate was dried at 60°C and assay was prepared, read at 560 nm, and hydroxyproline content was calculated according to the manufacturer's instructions (MilliporeSigma).

Cell proliferation and colony formation assays

Cells were seeded onto 96-well plates at a density of $5-10 \times 10^3$ cells/well and cultured for the indicated treatment. Cell proliferation was evaluated using an MTS assay kit (Promega, Madison, WI, USA). Twenty microliters of the combined MTS/phenazine methosulfate solution was added into each well, incubated for 3 h at 37°C, and the absorbance was measured at 490 nm by using an ELISA reader. For Trypan blue test, cells were plated on 12-well plates and treated with the indicated chemotherapeutic agents. After 72 h, both attached and detached cells were collected and then stained with 0.2% Trypan blue (0.1% final concentration), and the number of Trypan blue–positive and negative cells was counted using a hemocytometer under low-power microscopy. For colony-forming assays, 200 cells were seeded in each well of the 6-well plates. IPF-1 or IPF-2 primary cells were treated with peptides at the indicated concentrations for 10 d. Colonies were stained using 0.001% crystal violet, and the number of colonies with a diameter >0.5 mm was counted under an inverted microscope.

Evaluation of therapeutic interactions

The therapeutic interactions between the multikinase inhibitor nintedanib and MPS peptide were evaluated according to the method of Chou and Talalay (36) with the help of the Calcusyn software suite (Biosoft, Cambridge, United Kingdom). Combination index (CI) values were determined by generating dose-response curves for various concentrations of nintedanib (0.625–20 μM) treatment in conjunction with MPS peptide (6.25–200 μM) and then calculated at different drug concentrations. According to Chou and Talalay, a CI of <1 indicates a synergistic interaction, a CI of 1 indicates an additive interaction, and a CI of >1 indicates an antagonistic interaction.

Statistical analysis

Data are presented as the means ± SD for at least 3 independent experiments. The quantitative *in vitro* and *in vivo* data were analyzed using the Student's *t* test. The difference in patient characteristics between the high-expression and low-expression groups was analyzed using Fisher's exact test. All analyses were performed using SPSS software (v.10.0; SPSS, Chicago, IL, USA). All statistical tests were 2-sided, and values of $P < 0.05$ were considered statistically significant.

RESULTS

Aberrant elevation of MARCKS expression and its relevance to IPF fibroblasts

To discover the regulators of IPF fibroblast activation, we compared and integrated the gene profiles of IPF fibroblasts from 2 different microarray platforms. Among the genes identified, MARCKS was found to be highly associated with the expression of the myofibroblast marker α-SMA and was notably overexpressed in IPF fibroblasts (unpublished results). Through the analysis of the transcriptome dataset (Wang X. M., Zhang Y., Kim H. P., Zhou Z., Feghali-Bostwick C. A., Liu F., Ifedigbo E, Xu X., Oury T. D., Kaminski N., and Choi A. M.) (37), we compared MARCKS gene expression between 15 samples obtained from surgical remnants of biopsies or lungs explanted from patients with IPF that underwent pulmonary transplant and 11 normal histology lung samples resected from patients with lung cancer. Data analyzed with the Wilcoxon/Mann-Whitney tests demonstrated that MARCKS mRNA levels were significantly higher in IPF lung tissues than in normal lung tissue sections (**Fig. 1*A***, $P < 0.05$). To validate that MARCKS is dysregulated in IPF fibroblasts, we examined MARCKS expression and its phosphorylation in primary lung fibroblast cells isolated from patients with IPF and those with non-IPF. Figure 1*B* shows

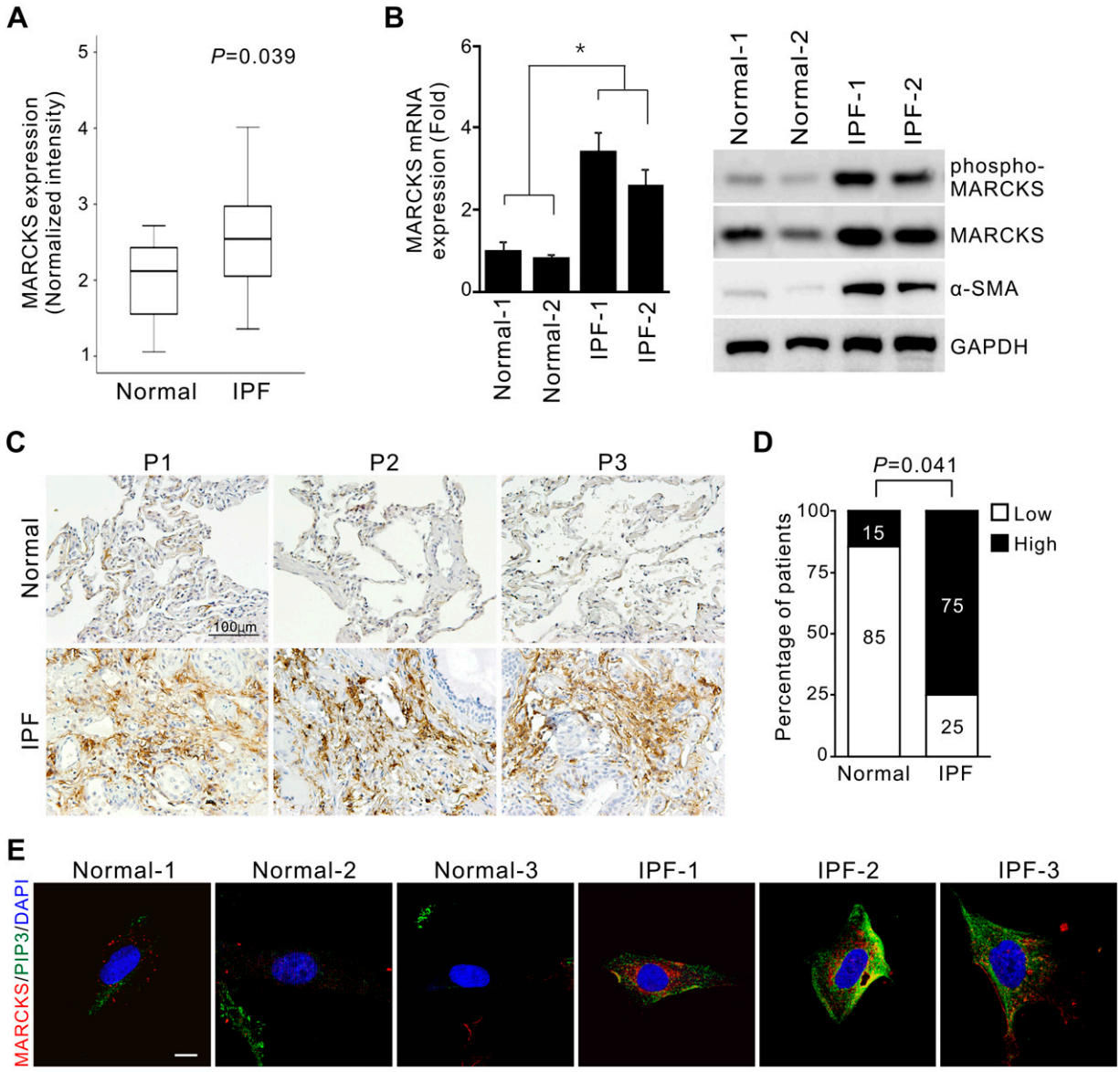

Figure 1. MARCKS is up-regulated in IPF. *A*) Normalized expression of MARCKS in IPF tissues ($n = 15$) *vs.* normal histology lung tissue samples ($n = 11$) using the GSE2052 dataset. *B*) Left: expression of MARCKS mRNA in primary normal fibroblasts (Normal-1 and -2) and primary IPF fibroblast cells (IPF-1 and IPF-2) as measured by real-time quantitative RT-PCR ($n = 5$). *$P < 0.05$ *vs.* Normal-1. Right: MARCKS protein and its phosphorylation was determined by Western blotting. *C*, *D*) Higher IHC staining of MARCKS protein in IPF tissues *vs.* normal lung tissue samples. *C*) Representative images utilizing anti-pSer159/163 MARCKS mAb in normal lung tissue ($n = 7$) and IPF specimens ($n = 8$) from patients. P1, P2, and P3 are 3 representative patients. Scale bar, 100 μm. *D*) Percentage of patients with high and low levels of phospho-MARCKS expression corresponding to normal and IPF. Numbers in bars represent the percentage of patients for each condition. *E*) Expression levels of MARCKS and PIP3 in 3 primary normal fibroblasts and IPF fibroblast cells as stained with anti-MARCKS and anti-PIP3 antibodies. The fluorescence of tetramethylrhodamine –conjugated MARCKS (red) and FITC-conjugated PIP3 (green) as well as nucleus counter-stained DAPI (blue) was visualized under a confocal laser-scanning microscope. Scale bar, 10 μm.

increased expression of MARCKS mRNA (left) and higher levels of phospho-MARCKS, MARCKS, and α-SMA (right) in 2 IPF fibroblast cells (IPF-1 -2) as compared with normal fibroblasts (Normal-1 and -2), suggesting the implications of high MARCKS expression in IPF fibroblasts.

Because MARCKS's function depends on its phosphorylation at Ser159 and Ser163, we next histologically confirmed phospho-MARCKS levels in both normal lung samples and IPF lung tissues from patients. IHC analysis of MARCKS phosphorylation showed an increase of phospho-MARCKS signals in the tissue sections from patients with IPF (Fig. 1*C*). We also found that higher levels of MARCKS phosphorylation occurred in IPF *vs.* normal tissues at 75 *vs.* 15%, respectively (Fig. 1*D*), and there was a positive correlation between phospho-MARCKS and IPF status (Fig. 1*D*, $P = 0.041$). Utilizing immunofluorescence and confocal microscopy, we observed detachment of MARCKS protein from the cell membrane occurred in primary IPF fibroblast cells, suggesting up-regulation of MARCKS phosphorylation in IPF

fibroblasts (Fig. 1*E*). We next quantified the above immunofluorescence signal intensity and we found that IPF fibroblasts expressed higher levels of PIP3 pools, as compared with primary normal fibroblasts (Fig. 1*E* and Supplemental Fig. S1*A*). Thus, phospho-MARCKS is likely of high importance in patients with IPF.

MARCKS inhibition down-regulates PIP3 production, AKT activity, and α-SMA expression

Given the importance of the PSD in the functionality of MARCKS protein, we previously developed the 25-mer MPS peptide to mimic the MARCKS PSD and showed that this peptide can directly inhibit phospho-MARCKS–mediated functions in cancers while having no cytotoxic effect on normal human bronchial epithelial cells (28, 30). Treatment with the MPS peptide in primary IPF fibroblast cells confirmed that this peptide had an inhibitory effect on MARCKS phosphorylation (**Fig. 2*A***), and this effect appeared to be dose- and duration-dependent. On the basis of the PIP2-binding motif on the MARCKS PSD, we first tested the effect of this peptide on PIP2 binding and PIP3 synthesis, which are the 2 major determinants for AKT activation (29). A kinetic assay confirmed that this peptide binds PIP2 with a dissociation constant of 17.64 nM (Fig. 2*B*). As expected, a decrease of PIP3 pools in MPS-treated IPF fibroblasts was observed (Fig. 2*C, D*), supporting the notion that MPS peptide is able to inhibit AKT activation by trapping PIP2. Indeed, Western blot analyses of phospho-AKT expression revealed concentration-dependent decrease of phospho-AKT levels in cultures treated with the MPS peptide but not in cultures treated with the scrambled peptide (**Fig. 3*A***).

To determine a causal effect of MARCKS inhibition on hallmarks of activated fibroblasts, we examined mRNA levels of COL1A1, FN1, THY1, VIM, and the most definitive molecular marker of myofibroblasts, α-SMA after treatment with MPS peptide. Treatment with MPS peptide in IPF fibroblast cells resulted in decreased levels of COL1A1 and fibronectin (Fig. 3*B, C* and Supplemental Fig. S2*A, B*). Strikingly, MPS-treated IPF fibroblast cells displayed significantly lower mRNA (Fig. 3*D*) and protein (Fig. 3*E*) expression of α-SMA as compared with cells receiving PBS or scrambled peptide. Because TGF-β is a major profibrogenic factor for α-SMA induction, primary normal lung fibroblasts were either treated with TGF-β alone or cotreated with TGF-β and MPS peptide. After 48 h, TGF-β treatment promoted expression of α-SMA and phospho-AKT abundance, whereas TGF-β–induced α-SMA expression was inhibited in the presence of MPS peptide (Supplemental Fig. S2*C*). Altogether, these data suggest an association of the MARCKS PSD with AKT activation and with myofibroblast differentiation.

MPS treatment suppresses IPF fibroblast activation *in vitro*

Based on the above molecular findings, we next examined whether MPS peptide inhibits the important determinants of fibrosis progression including cell proliferation, invasion, and migration. Two primary IPF fibroblast cells (IPF-1 and IPF-2), 1 IPF fibroblast cell line (LL97A), and primary normal fibroblast cells (Normal-1) were treated with various doses of MPS peptide for 72 h. Remarkably, impaired cell proliferation was noted in MPS-treated fibroblast cells with only a slight decrease of cell viability observed in normal cells (**Fig. 4*A***). In addition, data from Trypan blue exclusion test indicated that cell viability was significantly lower with 50 μM MPS treatment as compared with PBS or scrambled peptide group (Fig. 4*B*). We also observed a dose-dependent decrease of colony-forming ability in cells exposed to MPS peptide (Fig. 4*C*). Cell invasiveness in Matrigel-coated Transwells was also suppressed in the primary IPF fibroblasts, IPF-1 and IPF-2 cells, after MPS peptide treatment, whereas no suppression was seen with scrambled peptide treatment (Fig. 4*D*). Treatment of the primary IPF fibroblast cells with MPS at 100 μM reduced cell motility, as observed in wound-healing assays at 12 and 24 h postwound (Fig. 4*E*). We also used a MARCKS-shRNA to deplete endogenous MARCKS to determine whether an increase in phospho-MARCKS or total MARCKS abundance promotes cell motility of lung fibroblasts. As shown in Supplemental Fig. S3*A*, silencing MARCKS expression in high MARCKS-expressing fibroblast cells resulted in reducing cell migration, as compared with control shRNA-transduced cells.

The PI3K/AKT pathway participates in multiple complex signaling cascades, but PI3K inhibitors have had lackluster results thus far (38) when taken into clinical use. To further confirm the cytotoxicity of PI3K inhibition, we treated both types of cells with the PI3K inhibitor LY2940002. Unlike the selective effect observed with MPS on cells, the PI3K inhibitor exhibited a similar half maximal inhibitory concentration between IPF and normal fibroblast cells: 1262 nM in IPF-1 cells, 1088 nM in IPF-2 cells, and 745 nM in Normal-1 cells. These results demonstrate that MPS peptide has a suppressive activity on cell proliferation, invasion, and migration in IPF fibroblasts but not in normal fibroblast cells.

MPS peptide potentially serves as an antifibrotic agent in a bleomycin-induced pulmonary fibrosis

To translate our findings from *in vitro* into *in vivo*, we carried out the bleomycin-induced pulmonary fibrosis mouse model: 8-wk-old C57BL/6J mice received saline or bleomycin intratracheally as previously described (35). Lung specimens from C57BL/6J mice with either intratracheal administration of bleomycin (33 μg in 50 μl of saline) or saline were collected at d 21 after last bleomycin application. The paraffin-embedded lung sections were subjected to immunofluorescence staining by using anti–phospho-MARCKS and anti–α-SMA antibodies (**Fig. 5*A***). Data from immunofluorescence staining demonstrate elevated coexpression of phospho-MARCKS and α-SMA in bleomycin-treated lung tissues compared with those in the saline control (Fig. 5*B*), suggesting

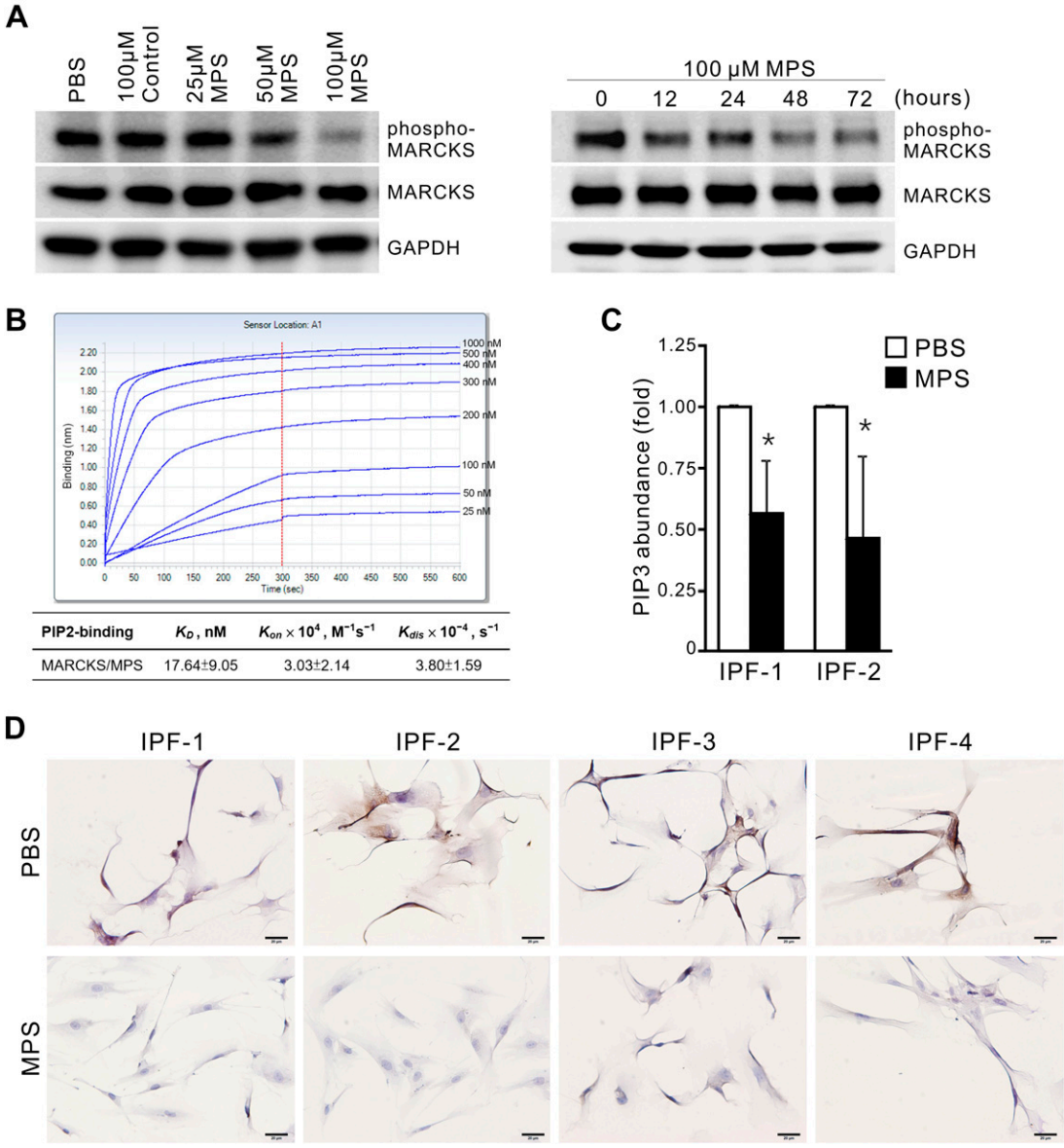

Figure 2. The mimetic of MARCKS, MPS peptide, targets phospho-MARCKS, binds to PIP2, and inhibits production of PIP3 pools. *A*) MPS peptide treatment inhibited MARCKS phosphorylation of primary IPF fibroblast cells. Left: cells were exposed to either 100 μM control peptide or 25–100 μM MPS peptide for 48 h and then subjected to Western blot analysis. Right: Western blot analysis of phospho-MARCKS levels in IPF fibroblasts after MPS treatment for 0, 12, 24, 48, and 72 h. *B*) Biolayer interferometry analysis of the binding of the MPS peptide to biotin-labeled PIP2. *C*) PIP3 levels in primary IPF fibroblast cells. $^*P < 0.05$ *vs.* control PBS (means ± SD). *D*) Multiple primary IPF fibroblasts were exposed to either PBS or 100 μM MPS peptide for 12 h and subjected to immunocytochemistry using anti-PIP3 antibody. GAPDH, glyceraldehyde 3-phosphate dehydrogenase. Representative images are shown ($n = 3$). Scale bars, 20 μm.

the potential role of phospho-MARCKS abundance in myofibroblast cells and pulmonary fibrosis. Next, lung fibroblast cells isolated from saline- or bleomycin-treated mice were incubated with either PBS or 100 μM MPS peptide for 72 h. Fibroblasts from bleomycin-treated mice exhibited a decrease in phospho-MARCKS, phospho-AKT, and α-SMA expression in the presence of MPS (Fig. 5C). Moreover, 3-(4,5-dimethylthiazol-2-yl)-2,5-diphenyltetrazolium bromide (MTT) assays confirmed that MPS treatment is very effective in decreasing cell viability of these fibroblast cells, as compared with the treatment of fibroblast cells from saline-treated mice (Fig. 5*D*).

Furthermore, we tested the feasibility of the MPS peptide as an antifibrotic agent in the bleomycin-induced pulmonary fibrosis mouse model. Upon bleomycin exposure for 9 d, the body weight of mice was obviously decreased, as compared with mice receiving saline (control group). Saline- and bleomycin-exposed mice then were treated with either PBS or MPS peptide intraperitoneally. To ascertain the therapeutic effect of MPS peptide on pulmonary fibrosis, MPS was administered intraperitoneally during the fibrotic phase of the model. **Figure 6*A*** illustrates the protocol for MPS administered in this study. In total, there were 4 groups (5 mice/group): *1*) saline plus PBS; *2*) saline plus MPS; *3*) bleomycin plus PBS;

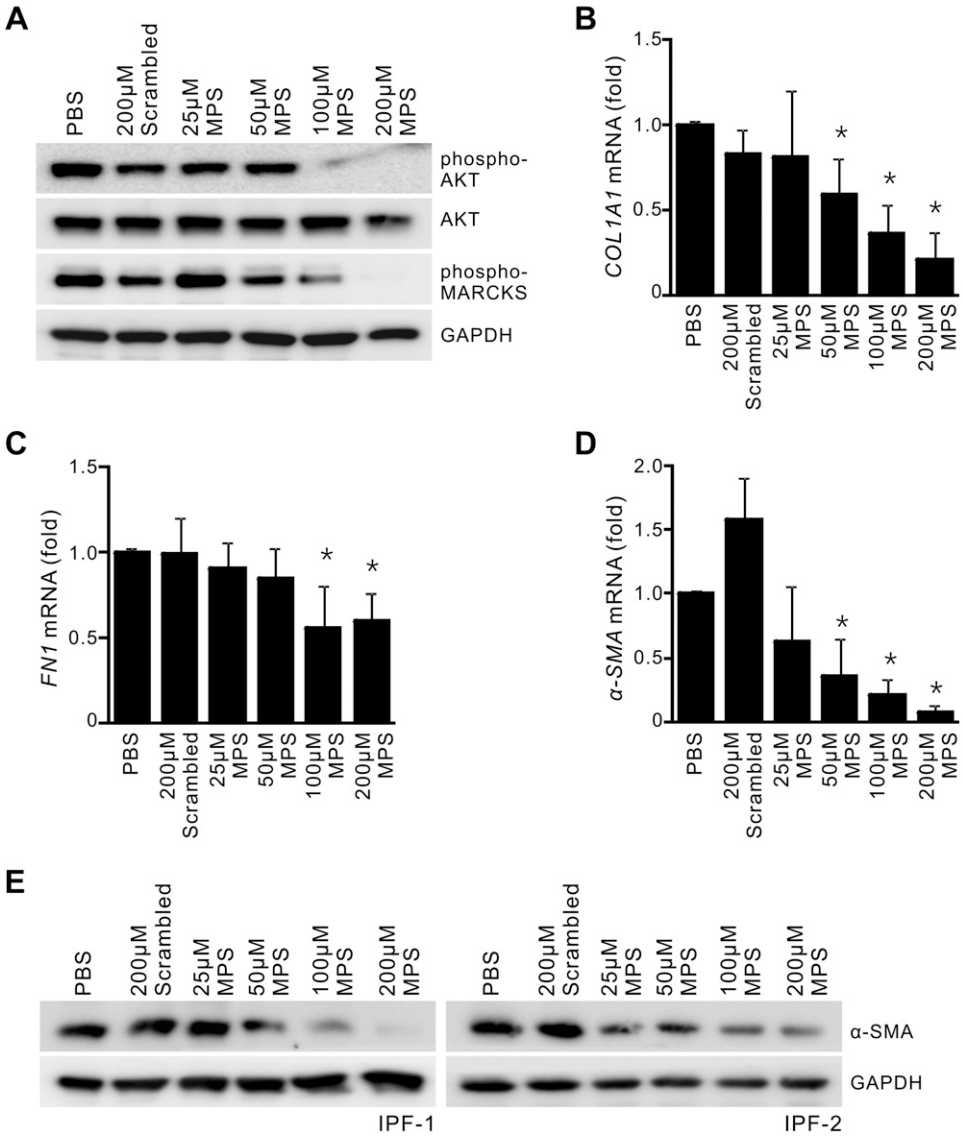

Figure 3. Targeting phospho-MARCKS by MPS peptide suppresses AKT activation and myofibroblast-associated gene expression. *A*) Primary IPF fibroblasts, IPF-1 cells, were incubated in a medium containing 200 μM scrambled or various dosages of MPS peptide for 48 h and harvested for Western blotting. *B–D*) Myofibroblast-associated gene expression, including COL1A1 (*B*), FN1 (*C*), and α-SMA (*D*) in MPS-treated IPF fibroblasts. Cells from near-confluent cultures were harvested for RNA isolation, and the level of expression was quantified with real-time quantitative RT-PCR and expressed as fold change relative to PBS-treated cells ($n = 4$). *E*) α-SMA protein level was confirmed by Western blotting. GAPDH, glyceraldehyde 3-phosphate dehydrogenase. A representative example of 3 independent experiments is shown. $^*P < 0.05$.

and *4*) bleomycin plus MPS. Surprisingly, we found a continued loss of body weight in the mice exposed to bleomycin plus PBS but not in the bleomycin-exposed mice with MPS treatment (Fig. 6*B*). After 22 d of bleomycin exposure, mice lungs were collected and processed for histology and collagen content analysis. Bleomycin-exposed mice showed extensive structural changes in the lungs, whereas decreases of both fibroblastic lesions and deposited ECM were seen in the lungs from these mice with bleomycin exposure and MPS treatment (Fig. 6*C*). In an attempt to compare the antifibrotic effects between MPS peptide and nintedanib, the currently FDA-approved therapeutic agent for IPF, we conducted the other cohort of bleomycin-induced pulmonary fibrosis studies. These bleomycin-exposed mice were intraperitoneally injected with nintedanib (28 mg/kg) or MPS peptide (28 mg/kg) every 2 d for 7 injections ($n = 6$ mice/group). IHC staining showed a concomitant decrease of phospho-MARCKS and phospho-AKT levels in bleomycin-exposed lung tissues receiving MPS (Fig. 6*D*). Down-regulated levels of hydroxyproline were seen in the lungs from the bleomycin plus MPS group (Fig. 6*E*). These results suggest a potential therapeutic application of MPS peptide in the treatment of pulmonary fibrosis.

Synergistic antitumor efficacy of a multikinase inhibitor and MARCKS inhibition

The potent multikinase inhibitor nintedanib was documented to show antifibrotic and anti-inflammatory effects (7, 8). However, we observed an increase of α-SMA protein upon nintedanib treatment (**Fig. 7*A***) in IPF fibroblast cells, which agrees with the recent report that nintedanib induces α-SMA (39). We also confirmed a significant increase in mRNA expression of α-SMA but a decrease of FN1 mRNA levels in nintedanib-treated cells (Supplemental Fig. S4). Surprisingly, there was no change in phospho-AKT levels after nintedanib treatment (Fig. 7*B*). On the contrary, treatment with MPS peptide

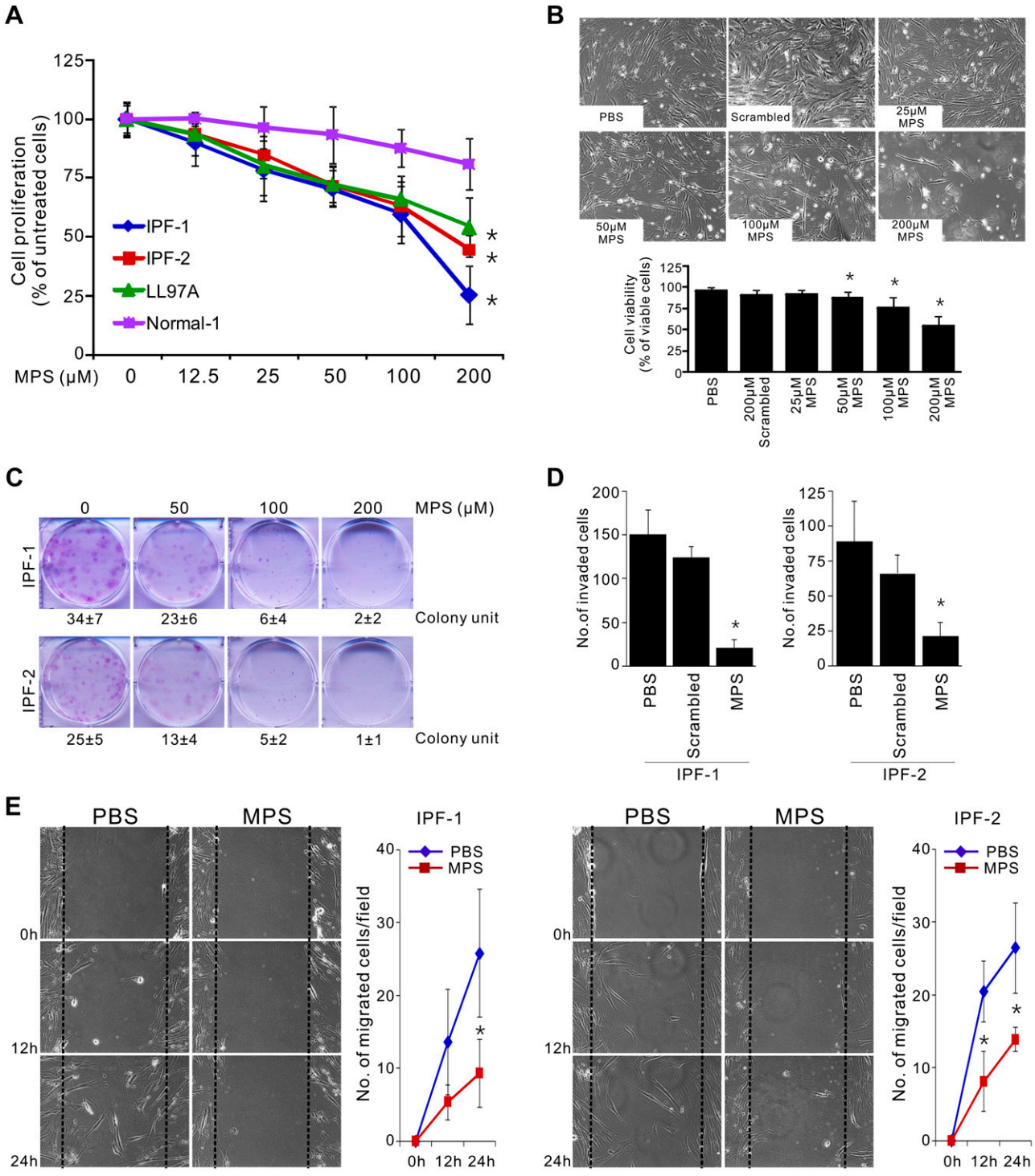

Figure 4. MPS peptide treatment impairs cell proliferation, invasiveness, and migration of primary IPF fibroblasts. *A*) Cells were incubated with various concentrations of the MPS peptide for 72 h and then subjected to MTS proliferation assays. *B*) IPF-1 cells were exposed to either 200 μM scrambled peptide or 25–200 μM MPS peptide. After 72 h, cell morphology (top) was photographed and cell viability (bottom) was determined by Trypan blue exclusion assay ($n = 6$). Cell viability was calculated by the number of viable cells/the number of total cells × 100. *C*) Cells were treated with the indicated concentrations of MPS peptide, and colonies were counted after 9 d using crystal violet staining. Top, data are representative of 3 independent experiments. Bottom, colony units (n) (means ± SD). *D*) Invasion ability of cells with or without MPS peptide as determined by Matrigel invasion assays. Dissociated cells of IPF-1 and -2 cultures were plated on Transwells with PBS, scrambled, or MPS peptide (100 μM), 20 h later, cells that migrated to the lower chamber were fixed, stained, and counted using light microscopy. Migrated cells to the lower chamber were quantified. Data expressed as means ± SD ($n = 4$). *$P < 0.05$ compared with PBS. *E*) Scratch/wound-healing assay for evaluating the inhibitory effects of MPS peptide on cell migration. Confluent cultures of IPF-1 and IPF-2 cells were scratched and wound-healing repair was monitored microscopically at 12 and 24 h after the scratch with and without addition of MPS peptide (100 μM). Left: phase contrast pictures. Right: numbers of cells migrated to the wound area were quantified at 12 and 24 h postscratching ($n = 4$). *$P < 0.05$ *vs.* PBS. Data are representative of 3 independent experiments.

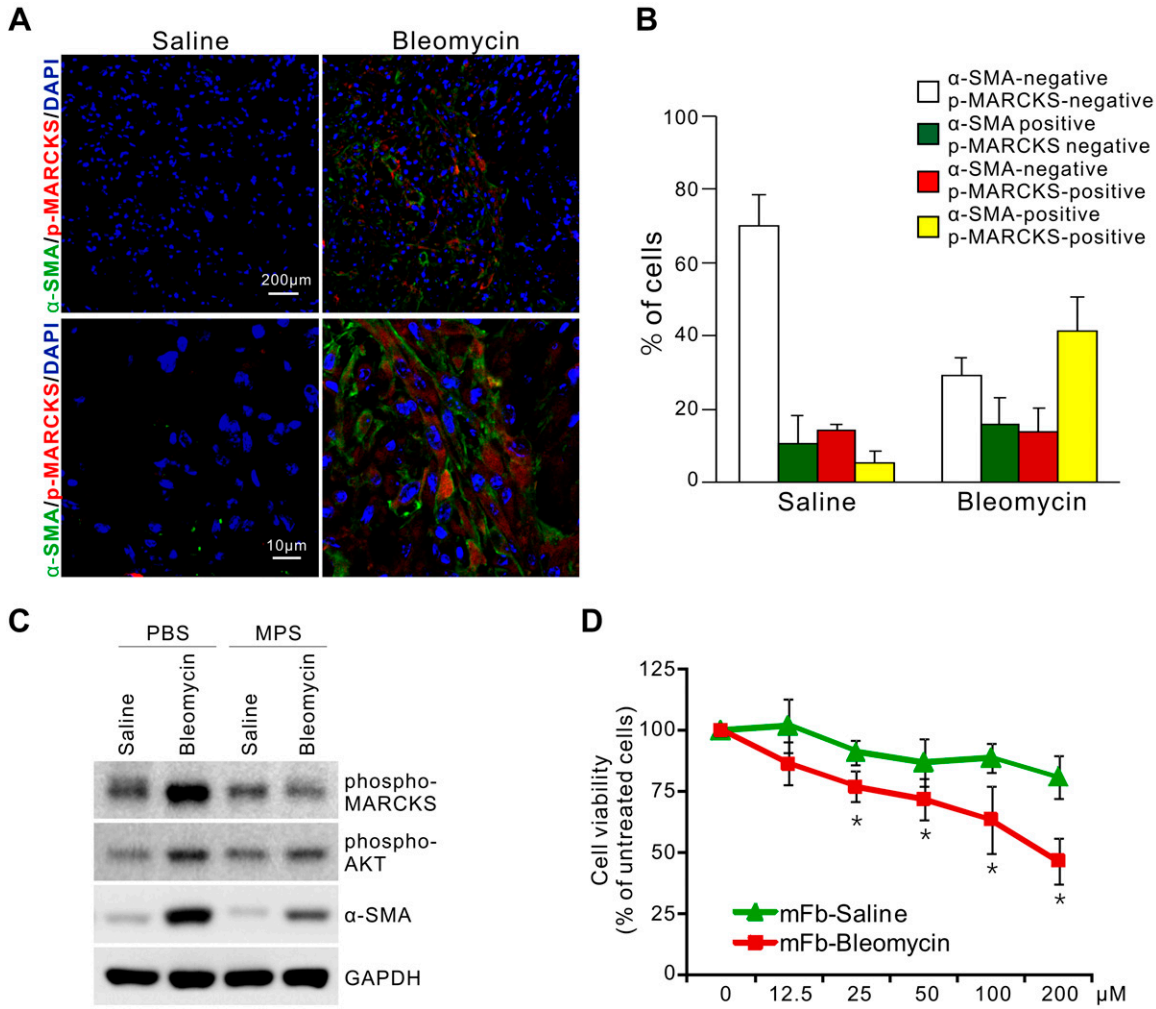

Figure 5. MPS peptide has an inhibitory effect on cell viability of α-SMA–expressing murine fibroblasts. *A*) Representative images of immunofluorescence staining of phospho-MARCKS (red color) and α-SMA (green color) in lung tissues from mice exposed to saline or bleomycin. DAPI (blue color): nucleus stains. *B*) Quantification of phospho-MARCKS– and α-SMA–positive staining cells (means ± SD, $n = 3$). *C*) Western blots analysis of phospho-MARCKS, phospho-AKT, and α-SMA expression in lung fibroblast cells isolated from saline- or bleomycin-treated mice after 48 h of treatment with 100 μM control or MPS peptide. *D*) Effect of MPS peptide on cell viability of lung fibroblasts isolated from saline- (mFb-Saline) or bleomycin-treated (mFb-Bleomycin) mice using MTT assays ($n = 4$). GAPDH, glyceraldehyde 3-phosphate dehydrogenase. $^*P < 0.05$.

decreased both phospho-AKT and α-SMA expression. The combination treatment of MPS peptide and nintedanib on IPF fibroblasts showed that MPS peptide has an inhibitory effect on nintedanib-enhanced α-SMA expression. Given the effect of MPS peptide on reducing phospho-AKT and α-SMA levels, we hypothesized that MARCKS inhibition by MPS treatment may improve nintedanib efficacy. To this end, the primary fibroblast cells were treated with various doses of nintedanib (62.5–2000 nM) and/or MPS peptide (6.25–200 μM) for 72 h. After either single or combination treatment, cell viability was decreased in IPF-1 (Fig. 7*C*) and IPF-2 (Fig. 7*D*) cells when treated with either nintedanib, the MPS peptide, or a combination of both drugs, with the greatest inhibition of viability observed in the combination group.

To evaluate the therapeutic interactions between nintedanib and MPS peptide, we used the Chou and Talalay CI method (36), and we demonstrated that the addition of MPS substantially enhanced the viability suppression of nintedanib with a CI value ~0.5 at ED_{50} (CI < 1), indicating the synergistic effect of drug combination (Fig. 7*E*). Particularly, the values were lower than 1 at ED_{50}, ~1 at ED_{75}, and above 1 at ED_{90} (unpublished results). Thus, the combination effect was dose-dependently correlated with the components, and therefore low-dose nintedanib in combination with a low dose of MPS presents a synergistic effect on cell proliferation. Simultaneously, data from Trypan blue exclusion test indicated that cell survival was significantly lower with the combination treatment as compared with control, MPS, and nintedanib (Fig. 7*F*). These data convincingly demonstrate that MPS treatment enhances nintedanib efficacy in IPF fibroblast cells and represents a viable and novel option for patients with IPF.

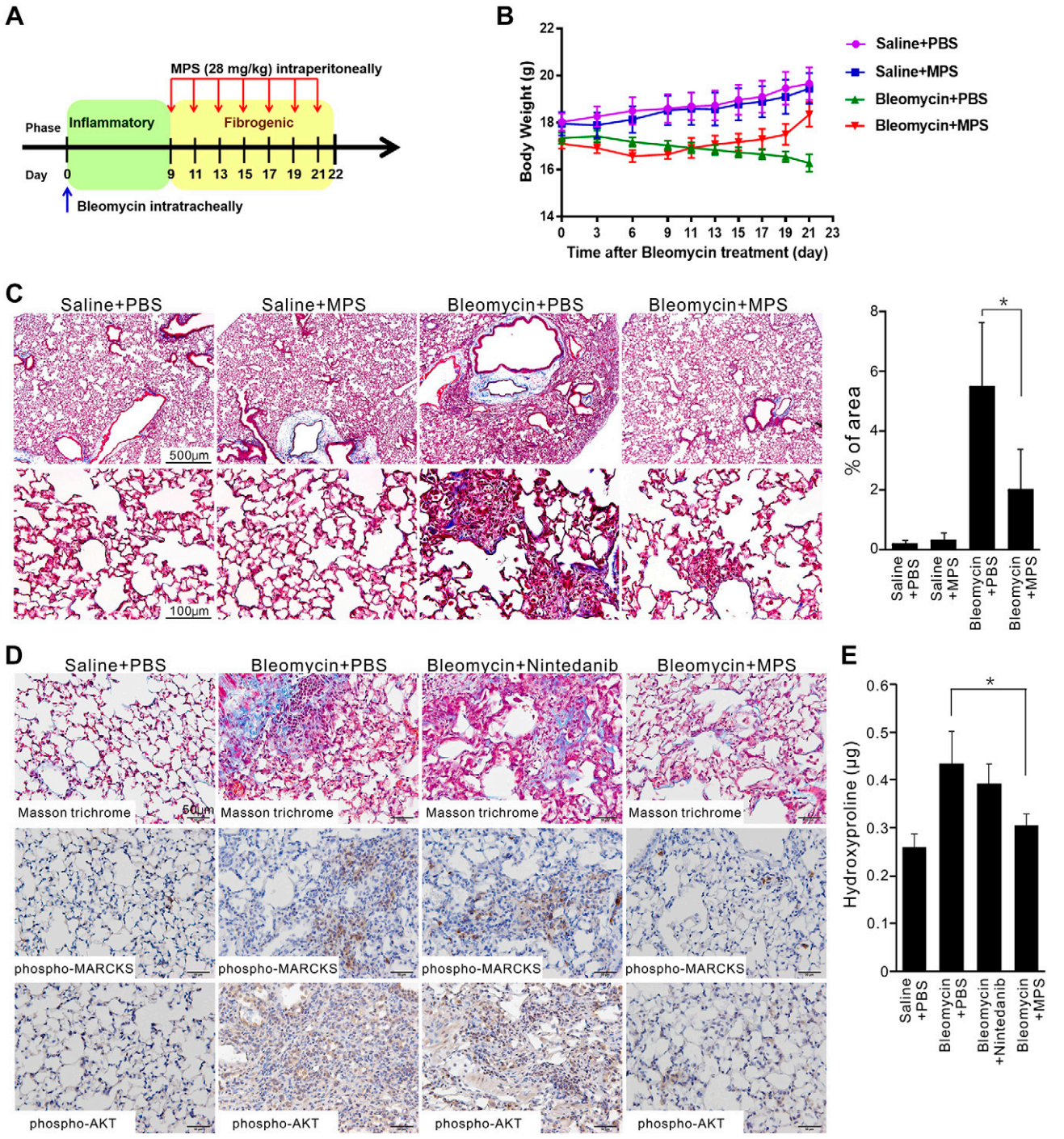

Figure 6. Suppressive effects of MPS peptide on pulmonary fibrosis *in vivo*. *A–C*) C57BL/6 mice were intraperitoneally given either PBS or MPS peptide at a dosage of 28 mg/kg every 2 d after mice intratracheally received 1 shot of saline or bleomycin (33 μg in 50 ml of saline, $n = 5$). Sequence of events (*A*) and body weight of mice (*B*) in bleomycin-induced pulmonary fibrosis with and without MPS treatment. *C*) Left: representative Masson trichrome–stained sections of mouse lung with various treatments. Original magnification: ×4 (top); ×20 (bottom). Right: semiquantitative fibrosis score from Masson trichrome–stained sections of mouse lung. Fibrosis score is expressed as the percentage of positive staining area per high-powered field. Analysis of 6–12 high-powered fields per lung was performed with ImageJ software. $^*P < 0.05$. *D*, *E*) Bleomycin-exposed mice were intraperitoneally given either nintedanib or MPS treatment at the dosage of 28 mg/kg every 2 d. *D*) Representative Masson trichrome and IHC staining of phospho-MARCKS (Ser159/163) and phospho-AKT (Ser473) ($n = 6$). *E*) Hydroxyproline level in the left lung of mice as described above was determined by a hydroxyproline ELISA assay (means ± SD). $^*P < 0.05$.

DISCUSSION

IPF is a progressive fibrotic lung disease characterized by unregulated proliferation of fibroblasts and excessive ECM deposition. In our current work, we have identified MARCKS as a novel α-SMA regulator. We observed increased levels of phospho-MARCKS in clinical IPF lung tissues, in primary fibroblasts *in vitro*,

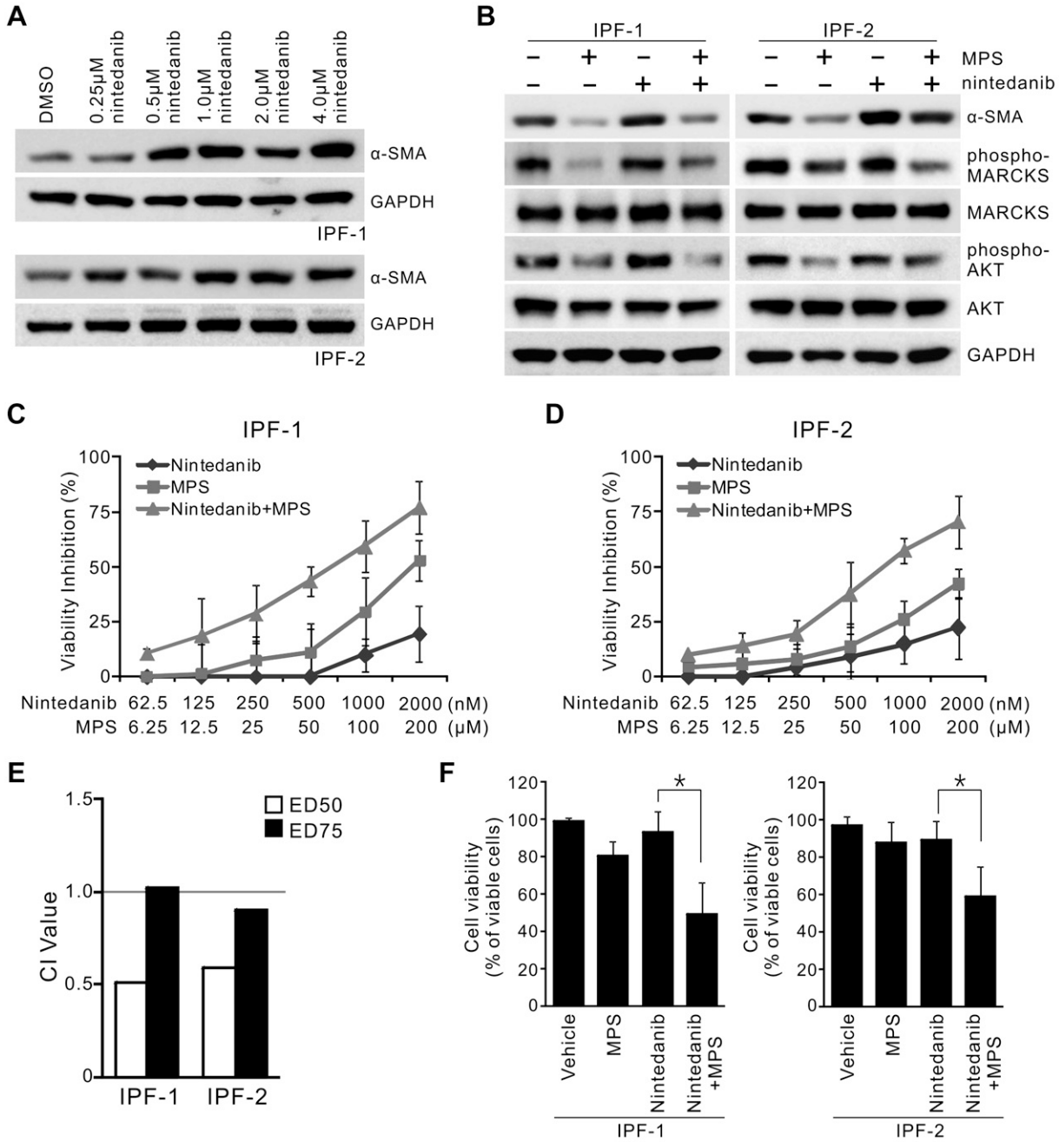

Figure 7. MPS peptide acts synergistically with nintedanib in IPF. *A*) Nintedanib treatment induces α-SMA protein expression in primary IPF fibroblasts. Cells were incubated with various doses of nintedanib as indicated. After 48 h, cells were collected and subjected to Western blot analysis. *B*) Western blot analysis of α-SMA, phospho-MARCKS, and phospho-AKT in primary IPF fibroblasts with nintedanib (1000 nM) and/or MPS (100 μM) for 48 h. *C–E*) Combinatorial effect of MPS peptide with nintedanib on fibroblasts isolated from 2 patients with IPF. *C, D*) Cells were treated with various doses of nintedanib (62.5–2000 nM) and/or MPS peptide (6.25–200 μM) for 72 h, respectively. After single (blue/red line) or combined (green line) treatment, cell viability was determined by MTT assays. *E*) The Chou and Talalay CI method was utilized to evaluate the therapeutic interactions between nintedanib and MPS peptide using the Calcusyn software. Gray line, additive effect of the combination of MPS peptide and the drug is represented at CI = 1. *F*) Cells were individually treated with 1 μM nintedanib, 100 μM MPS peptide, or combinations of 1 μM nintedanib and 100 μM MPS peptide. After 48 h, cell viability was determined by the Trypan blue exclusion assay ($n = 3$). GAPDH, glyceraldehyde 3-phosphate dehydrogenase. $^*P < 0.05$.

and in bleomycin animal models correlated with α-SMA expression (Figs. 1 and 5). Additionally, attenuation of phospho-MARCKS through MPS peptide reduced α-SMA simultaneously with phospho-AKT *in vitro* and *ex vivo* (Figs. 3 and 5). Inhibition of phospho-MARCKS also reduced myofibroblast migration ability and survival *in vitro*, attenuated fibrosis in the animal model (Figs. 4 and 6), as well as down-regulated COL1A1 expression on the transcriptional level. Lastly, we examined the effects of MPS

peptide treatment in conjunction with nintedanib treatment and observed marked reduction in α-SMA correlated with reduction in phospho-MARCKS and phospho-AKT (Fig. 7). Taken together, these findings suggest a novel role of MARCKS in IPF fibrogenesis and offers a potential marker and promising therapeutic target.

The histopathologic lesions in IPF are dominated by the presence of increased ECM proteins (type I collagen–rich) and accumulation of fibroblasts, which are the key effector cells in fibrosis development (18, 40). Unlike quiescent or resting fibroblasts, the majority of lung fibroblasts from patients with IPF display an abnormally "activated" phenotype, namely pathologic alterations in proliferation, migration, and differentiation into myofibroblasts (41–43). The activated fibroblasts persist and proliferate, continuing to produce collagen, which disrupts the normal lung architecture. In light of the importance of activated fibroblasts in IPF progression, the signaling molecules regulating fibroblast proliferation, migration, and differentiation are coming into our focus. Herein, we identified phospho-MARCKS as a candidate target for regulating fibroblast activation. Our data showed a dramatic increase in phospho-MARCKS levels in both IPF lung tissue sections and primary fibroblast cells, indicating the clinical implications of increased phospho-MARCKS (MARCKS activation) in pulmonary fibrosis.

Indeed, lung fibroblasts derived from patients with IPF displayed up-regulation of phospho-MARCKS and MARCKS expression, which are highly associated with expression of α-SMA, a myofibroblast marker. Down-regulation of phospho-MARCKS led to the suppression of fibroblast cell proliferation, migration, and/or myofibroblast differentiation (α-SMA expression). Because phospho-MARCKS has been demonstrated to play a role in lung cancer cell proliferation, invasion, and migration (27, 28), it is logical that phospho-MARCKS, and manipulation thereof, would have similar effects on fibroblasts. Although MARCKS has been extensively studied in many lung diseases, the functional role of MARCKS has not been explored in IPF and lung fibroblasts. To the best of our knowledge, this is the first study on the efficacy of MPS as an antifibrotic agent in IPF, and our results present MARCKS as a druggable target in this disease.

Targeting both increased fibroblast proliferation and myofibroblast differentiation has been considered as a therapeutic strategy in IPF management; however, the detailed mechanism of fibrosis remains unclear, and effective treatment options remain limited (1–3, 5, 12, 13, 44). Although a few signaling proteins influencing fibroblast activation and/or myofibroblast differentiation, such as PDGFR, FGFR, VEGFR, TGF-β, and PI3K, have been identified (9, 10, 21, 22, 45), the mechanisms behind fibrotic disorders are still incomplete. Currently, 2 FDA-approved drugs that target the above pathways for IPF are pirfenidone and nintedanib (30, 44). Although effective at slowing progression, these drugs are unable to completely stop or reverse progression. Additionally, the exact mechanism of action for pirfenidone is unknown, and these drugs also come with a plethora of detrimental side effects that necessitate stopping treatment in the affected patients (4, 7, 12, 13, 46). Additionally, we have observed that the PI3K/AKT pathway is still active after nintedanib treatment *in vitro*, suggesting that the drug is ineffective at inhibiting PI3K/AKT activity. Despite having a defined mode of action, the array of side effects and insufficient blocking of AKT activity makes nintedanib an inadequate therapeutic for IPF.

A previous study by Rangarajan *et al.* (39) suggested that nintedanib treatment up-regulates α-SMA expression in fibroblasts. In agreement with this finding, we also observed an increase of α-SMA expression in lung fibroblasts of the patient with IPF after treatment with nintedanib. Although nintedanib has shown effectiveness in reducing fibroblast cell proliferation and migratory ability (7), it is not able to reduce phospho-AKT and increases α-SMA on a transcriptional level. This suggests that although nintedanib may be effective at slowing fibroblast cell proliferation and motility, there are alternative pathways that are still active, leading to continued progression, perhaps offering an explanation as to why nintedanib alone does not stop IPF progression. One such active pathway is the TGF-β/AKT/α-SMA axis. We demonstrate that this axis is activated in response to TGF-β stimulation in lung fibroblasts, leading to an up-regulated level of α-SMA and phospho-AKT. The MPS peptide can target this activation, resulting in decreased α-SMA and reduced phospho-AKT activity (Supplemental Fig. S2*C*). These findings indicate that targeting the TGF-β pathway through attenuating PI3K/AKT activity *via* PIP2 sequestration is an effective approach to addressing TGF-β-mediated myofibroblast differentiation and activity.

In conjunction with associated adverse side effects, there is a clear need to improve drug efficacy. In order to tackle this problem, we implemented the novel use of nintedanib in combination treatment in IPF fibroblasts. Combination therapy itself is not a novel concept as it has been effectively employed in the treatment of various cancer types. However, the use of combination therapy is limited in IPF, and many combined treatments do not offer significant improvements to IPF progression and survival (46–49). In our study, we have shown that the combination of nintedanib with MPS peptide has shown a synergistic effect on attenuating myofibroblast survival, proliferation, and migration, especially at lower concentrations. This is potentially due to the combinatorial effect of targeting VEGFR, FGFR, and PDGFR in compliment with targeting TGF-β activity. Although nintedanib has been demonstrated to target the downstream activities of VEGFR, FGFR, and PDGFR (7), the TGF-β pathway is not sufficiently targeted by this inhibitor. The addition of MPS peptide in conjunction with nintedanib treatment allows for more comprehensive attenuation of TGF-β and AKT activity in lung fibroblasts (Figs. 5*C* and 7*B* and Supplemental Fig. S2*C*). This presents itself as a promising approach to the treatment of IPF as lower dosages of therapeutics could be achieved, thus potentially mitigating side effects while improving IPF outcomes.

There is mounting evidence pointing to the importance of the PI3K/AKT pathway in fibrosis progression through promoting myofibroblast survival, migration, and proliferation (20–23, 45, 50, 51). Given that MARCKS plays a critical role in the regulation of PI3K and subsequent AKT activity through modulating PIP2 pools (27–29), we hypothesized a correlation between the PI3K pathway and phospho-MARCKS abundance in the context of IPF fibroblast activation. MARCKS interacts with PIP2 at the cell membrane through electrostatic interactions at the PSD (52). In an unphosphorylated state, MARCKS sequesters PIP2 pools *via* the PSD; however, after PSD phosphorylation, MARCKS disassociates from the membrane and exposes PIP2 to PI3K. Previously, we have demonstrated the interaction between PI3K and MARCKS in a panel of lung cancer cells (28). Targeting MARCKS is an appealing approach as PIP2 to PIP3 synthesis is a universal step in PI3K signaling. In both bleomycin animal models and *in vitro* assays, we observed increased phospho-MARCKS levels in IPF fibroblasts or in fibroblasts isolated from bleomycin-treated mice. Treatment with the MPS peptide targeting the MARCKS PSD (28) in various IPF fibroblasts confirmed that this peptide had an inhibitory effect on MARCKS phosphorylation, AKT activity, cell proliferation, colony formation, invasiveness, and motility, which is consistent with our previous findings in cancers (28, 30). Additionally, we found that attenuation of phospho-MARCKS significantly reduces the expression of myofibroblast marker α-SMA and fibrotic marker collagen. Importantly, the *in vivo* results are consistent with the above *in vitro* findings and support the notion that the 25-mer peptide targeting the MARCKS PSD sequence, MPS, has therapeutic applications as a novel antifibrotic agent.

Targeting MARCKS and its signaling axis through the use of MPS peptide to abrogate myofibroblasts, both *in vitro* and *in vivo*, serves as a proof of concept for suppressing IPF progression. Currently, a large number of potential antifibrotic compounds are given as preventive treatment in preclinical studies; as a result, the translation of these findings into clinical practice has not been very successful (46, 53, 54). To better reflect the management of human IPF and to reveal beneficial compounds, we evaluated the antifibrotic properties of the MPS peptide in the phase of established fibrosis in mice. We believe the therapeutic potential of this novel peptide in bleomycin-induced pulmonary fibrosis was demonstrated for the first time and will contribute to development of treatments that destroy activated fibroblasts without adversely affecting quiescent fibroblasts.

In summary, our results suggest phospho-MARCKS as a promising therapeutic target in IPF. As TGF-β signaling is not completely blocked by multikinase inhibitors such as nintedanib, the PI3K/AKT pathway is still active in myofibroblasts in IPF. Attenuation of MARCKS, an upstream regulator of PI3K, *via* MPS peptide was shown to reduce fibrotic markers and fibrosis both *in vitro* and *in vivo*. Furthermore, we have shown combination treatment of MPS peptide and nintedanib to be an effective and promising approach in addressing the current lack of effective treatments. Taken together, we have shown MARCKS to be an important player and target, further elucidated the mechanisms involved in fibrosis, and introduced a novel and promising approach in the treatment of IPF. FJ

ACKNOWLEDGMENTS

The authors thank Dr. Richart Harper and Dr, Angela Linderholm [University of California–Davis (UC Davis)] for collection of lung tissue samples, and Lisa Franzi and Cameron Larson (UC Davis) for assistance with the experiments, as well as the UC Davis Comprehensive Cancer Center for pathology support. This work was supported by the California University of California Office of the President (UCOP) Tobacco-Related Disease Research Program (Grants TRDRP 27KT-0004 and 28IR-0061) and U.S. National Institutes of Health, National Heart, Lung, and Blood Institute Grant R01HL146802. The authors declare no conflicts of interest.

AUTHOR CONTRIBUTIONS

C.-H. Chen conceived and designed the experiments; D. C. Yang, J.-M. Li, J. Xu, and C.-H. Chen performed the experiments; D. C. Yang, J.-M. Li, J. Xu, and C.-H. Chen analyzed the data; J. Oldham, S. H. Phan, J. A. Last, R. Wu, and C.-H. Chen contributed reagents, materials and analysis tools; D. C. Yang, R. Wu, and C.-H. Chen wrote the paper; and all authors read and approved the final manuscript.

REFERENCES

1. Ley, B., Collard, H. R., and King, T. E., Jr. (2011) Clinical course and prediction of survival in idiopathic pulmonary fibrosis. *Am. J. Respir. Crit. Care Med.* **183**, 431–440
2. Nalysnyk, L., Cid-Ruzafa, J., Rotella, P., and Esser, D. (2012) Incidence and prevalence of idiopathic pulmonary fibrosis: review of the literature. *Eur. Respir. Rev.* **21**, 355–361
3. Raghu, G., and Richeldi, L. (2017) Current approaches to the management of idiopathic pulmonary fibrosis. *Respir. Med.* **129**, 24–30
4. Azuma, A., Nukiwa, T., Tsuboi, E., Suga, M., Abe, S., Nakata, K., Taguchi, Y., Nagai, S., Itoh, H., Ohi, M., Sato, A., and Kudoh, S. (2005) Double-blind, placebo-controlled trial of pirfenidone in patients with idiopathic pulmonary fibrosis. *Am. J. Respir. Crit. Care Med.* **171**, 1040–1047
5. Sköld, C. M., Bendstrup, E., Myllärniemi, M., Gudmundsson, G., Sjåheim, T., Hilberg, O., Altraja, A., Kaarteenaho, R., and Ferrara, G. (2017) Treatment of idiopathic pulmonary fibrosis: a position paper from a Nordic expert group. *J. Intern. Med.* **281**, 149–166
6. Taniguchi, H., Ebina, M., Kondoh, Y., Ogura, T., Azuma, A., Suga, M., Taguchi, Y., Takahashi, H., Nakata, K., Sato, A., Takeuchi, M., Raghu, G., Kudoh, S., and Nukiwa, T.; Pirfenidone Clinical Study Group in Japan. (2010) Pirfenidone in idiopathic pulmonary fibrosis. *Eur. Respir. J.* **35**, 821–829
7. Wollin, L., Wex, E., Pautsch, A., Schnapp, G., Hostettler, K. E., Stowasser, S., and Kolb, M. (2015) Mode of action of nintedanib in the treatment of idiopathic pulmonary fibrosis. *Eur. Respir. J.* **45**, 1434–1445
8. Wollin, L., Maillet, I., Quesniaux, V., Holweg, A., and Ryffel, B. (2014) Antifibrotic and anti-inflammatory activity of the tyrosine kinase inhibitor nintedanib in experimental models of lung fibrosis. *J. Pharmacol. Exp. Ther.* **349**, 209–220

9. Tatler, A. L., and Jenkins, G. (2012) TGF-β activation and lung fibrosis. *Proc. Am. Thorac. Soc.* **9**, 130–136
10. Fernandez, I. E., and Eickelberg, O. (2012) The impact of TGF-β on lung fibrosis: from targeting to biomarkers. *Proc. Am. Thorac. Soc.* **9**, 111–116
11. Rangarajan, S., Locy, M. L., Luckhardt, T. R., and Thannickal, V. J. (2016) Targeted therapy for idiopathic pulmonary fibrosis: where to now? *Drugs* **76**, 291–300
12. Richeldi, L., Costabel, U., Selman, M., Kim, D. S., Hansell, D. M., Nicholson, A. G., Brown, K. K., Flaherty, K. R., Noble, P. W., Raghu, G., Brun, M., Gupta, A., Juhel, N., Klüglich, M., and du Bois, R. M. (2011) Efficacy of a tyrosine kinase inhibitor in idiopathic pulmonary fibrosis. *N. Engl. J. Med.* **365**, 1079–1087
13. Richeldi, L., du Bois, R. M., Raghu, G., Azuma, A., Brown, K. K., Costabel, U., Cottin, V., Flaherty, K. R., Hansell, D. M., Inoue, Y., Kim, D. S., Kolb, M., Nicholson, A. G., Noble, P. W., Selman, M., Taniguchi, H., Brun, M., Le Maulf, F., Girard, M., Stowasser, S., Schlenker-Herceg, R., Disse, B., and Collard, H. R.; INPULSIS Trial Investigators. (2014) Efficacy and safety of nintedanib in idiopathic pulmonary fibrosis. *N. Engl. J. Med.* **370**, 2071–2082; erratum: 373, 782
14. Raghu, G., Collard, H. R., Egan, J. J., Martinez, F. J., Behr, J., Brown, K. K., Colby, T. V., Cordier, J. F., Flaherty, K. R., Lasky, J. A., Lynch, D. A., Ryu, J. H., Swigris, J. J., Wells, A. U., Ancochea, J., Bouros, D., Carvalho, C., Costabel, U., Ebina, M., Hansell, D. M., Johkoh, T., Kim, D. S., King, T. E., Jr., Kondoh, Y., Myers, J., Müller, N. L., Nicholson, A. G., Richeldi, L., Selman, M., Dudden, R. F., Griss, B. S., Protzko, S. L., and Schünemann, H. J.; ATS/ERS/JRS/ALAT Committee on Idiopathic Pulmonary Fibrosis. (2011) An official ATS/ERS/JRS/ALAT statement: idiopathic pulmonary fibrosis: evidence-based guidelines for diagnosis and management. *Am. J. Respir. Crit. Care Med.* **183**, 788–824
15. Martinez, F. J., Collard, H. R., Pardo, A., Raghu, G., Richeldi, L., Selman, M., Swigris, J. J., Taniguchi, H., and Wells, A. U. (2017) Idiopathic pulmonary fibrosis. *Nat. Rev. Dis. Primers* **3**, 17074
16. Katzenstein, A. L., and Myers, J. L. (1998) Idiopathic pulmonary fibrosis: clinical relevance of pathologic classification. *Am. J. Respir. Crit. Care Med.* **157**, 1301–1315
17. Kuhn, C., and McDonald, J. A. (1991) The roles of the myofibroblast in idiopathic pulmonary fibrosis. Ultrastructural and immunohistochemical features of sites of active extracellular matrix synthesis. *Am. J. Pathol.* **138**, 1257–1265
18. Wynn, T. A. (2011) Integrating mechanisms of pulmonary fibrosis. *J. Exp. Med.* **208**, 1339–1350
19. Leppäranta, O., Sens, C., Salmenkivi, K., Kinnula, V. L., Keski-Oja, J., Myllärniemi, M., and Koli, K. (2012) Regulation of TGF-β storage and activation in the human idiopathic pulmonary fibrosis lung. *Cell Tissue Res.* **348**, 491–503
20. Conte, E., Gili, E., Fruciano, M., Korfei, M., Fagone, E., Iemmolo, M., Lo Furno, D., Giuffrida, R., Crimi, N., Guenther, A., and Vancheri, C. (2013) PI3K p110γ overexpression in idiopathic pulmonary fibrosis lung tissue and fibroblast cells: in vitro effects of its inhibition. *Lab. Invest.* **93**, 566–576
21. Lu, Y., Azad, N., Wang, L., Iyer, A. K., Castranova, V., Jiang, B. H., and Rojanasakul, Y. (2010) Phosphatidylinositol-3-kinase/akt regulates bleomycin-induced fibroblast proliferation and collagen production. *Am. J. Respir. Cell Mol. Biol.* **42**, 432–441
22. White, E. S., Atrasz, R. G., Hu, B., Phan, S. H., Stambolic, V., Mak, T. W., Hogaboam, C. M., Flaherty, K. R., Martinez, F. J., Kontos, C. D., and Toews, G. B. (2006) Negative regulation of myofibroblast differentiation by PTEN (phosphatase and tensin homolog deleted on chromosome 10). *Am. J. Respir. Crit. Care Med.* **173**, 112–121
23. Horowitz, J. C., Lee, D. Y., Waghray, M., Keshamouni, V. G., Thomas, P. E., Zhang, H., Cui, Z., and Thannickal, V. J. (2004) Activation of the pro-survival phosphatidylinositol 3-kinase/AKT pathway by transforming growth factor-beta1 in mesenchymal cells is mediated by p38 MAPK-dependent induction of an autocrine growth factor. *J. Biol. Chem.* **279**, 1359–1367
24. Eckert, R. E., Neuder, L. E., Park, J., Adler, K. B., and Jones, S. L. (2010) Myristoylated alanine-rich C-kinase substrate (MARCKS) protein regulation of human neutrophil migration. *Am. J. Respir. Cell Mol. Biol.* **42**, 586–594
25. Green, T. D., Crews, A. L., Park, J., Fang, S., and Adler, K. B. (2011) Regulation of mucin secretion and inflammation in asthma: a role for MARCKS protein? *Biochim. Biophys. Acta* **1810**, 1110–1113
26. Park, J. A., Crews, A. L., Lampe, W. R., Fang, S., Park, J., and Adler, K. B. (2007) Protein kinase C delta regulates airway mucin secretion via phosphorylation of MARCKS protein. *Am. J. Pathol.* **171**, 1822–1830
27. Chen, C. H., Thai, P., Yoneda, K., Adler, K. B., Yang, P. C., and Wu, R. (2014) A peptide that inhibits function of Myristoylated Alanine-Rich C Kinase Substrate (MARCKS) reduces lung cancer metastasis. *Oncogene* **33**, 3696–3706
28. Chen, C. H., Statt, S., Chiu, C. L., Thai, P., Arif, M., Adler, K. B., and Wu, R. (2014) Targeting myristoylated alanine-rich C kinase substrate phosphorylation site domain in lung cancer. Mechanisms and therapeutic implications. *Am. J. Respir. Crit. Care Med.* **190**, 1127–1138
29. Ziemba, B. P., Burke, J. E., Masson, G., Williams, R. L., and Falke, J. J. (2016) Regulation of PI3K by PKC and MARCKS: single-molecule analysis of a reconstituted signaling pathway. *Biophys. J.* **110**, 1811–1825
30. Zhao, J., Shi, X., Wang, T., Ying, C., He, S., and Chen, Y. (2017) The prognostic and clinicopathological significance of IGF-1R in NSCLC: a meta-analysis. *Cell. Physiol. Biochem.* **43**, 697–704
31. Chen, B., Polunovsky, V., White, J., Blazar, B., Nakhleh, R., Jessurun, J., Peterson, M., and Bitterman, P. (1992) Mesenchymal cells isolated after acute lung injury manifest an enhanced proliferative phenotype. *J. Clin. Invest.* **90**, 1778–1785
32. Kuo, T. C., Tan, C. T., Chang, Y. W., Hong, C. C., Lee, W. J., Chen, M. W., Jeng, Y. M., Chiou, J., Yu, P., Chen, P. S., Wang, M. Y., Hsiao, M., Su, J. L., and Kuo, M. L. (2013) Angiopoietin-like protein 1 suppresses SLUG to inhibit cancer cell motility. *J. Clin. Invest.* **123**, 1082–1095
33. Chen, C. H., Chiu, C. L., Adler, K. B., and Wu, R. (2014) A novel predictor of cancer malignancy: up-regulation of myristoylated alanine-rich C kinase substrate phosphorylation in lung cancer. *Am. J. Respir. Crit. Care Med.* **189**, 1002–1004
34. Chen, C. H., Cheng, C. T., Yuan, Y., Zhai, J., Arif, M., Fong, L. W., Wu, R., and Ann, D. K. (2015) Elevated MARCKS phosphorylation contributes to unresponsiveness of breast cancer to paclitaxel treatment. *Oncotarget* **6**, 15194–15208
35. Limjunyawong, N., Mitzner, W., and Horton, M. R. (2014) A mouse model of chronic idiopathic pulmonary fibrosis. *Physiol. Rep.* **2**, e00249
36. Chou, T. C., and Talalay, P. (1984) Quantitative analysis of dose-effect relationships: the combined effects of multiple drugs or enzyme inhibitors. *Adv. Enzyme Regul.* **22**, 27–55
37. Wang, X. M., Zhang, Y., Kim, H. P., Zhou, Z., Feghali-Bostwick, C. A., Liu, F., Ifedigbo, E., Xu, X., Oury, T. D., Kaminski, N., and Choi, A. M. (2006) Caveolin-1: a critical regulator of lung fibrosis in idiopathic pulmonary fibrosis. *J. Exp. Med.* **203**, 2895–2906
38. Fruman, D. A., and Rommel, C. (2014) PI3K and cancer: lessons, challenges and opportunities. *Nat. Rev. Drug Discov.* **13**, 140–156
39. Rangarajan, S., Kurundkar, A., Kurundkar, D., Bernard, K., Sanders, Y. Y., Ding, Q., Antony, V. B., Zhang, J., Zmijewski, J., and Thannickal, V. J. (2016) Novel mechanisms for the antifibrotic action of nintedanib. *Am. J. Respir. Cell Mol. Biol.* **54**, 51–59
40. Bjoraker, J. A., Ryu, J. H., Edwin, M. K., Myers, J. L., Tazelaar, H. D., Schroeder, D. R., and Offord, K. P. (1998) Prognostic significance of histopathologic subsets in idiopathic pulmonary fibrosis. *Am. J. Respir. Crit. Care Med.* **157**, 199–203
41. Jordana, M., Schulman, J., McSharry, C., Irving, L. B., Newhouse, M. T., Jordana, G., and Gauldie, J. (1988) Heterogeneous proliferative characteristics of human adult lung fibroblast lines and clonally derived fibroblasts from control and fibrotic tissue. *Am. Rev. Respir. Dis.* **137**, 579–584
42. Raghu, G., Chen, Y. Y., Rusch, V., and Rabinovitch, P. S. (1988) Differential proliferation of fibroblasts cultured from normal and fibrotic human lungs. *Am. Rev. Respir. Dis.* **138**, 703–708
43. Sanders, Y. Y., Kumbla, P., and Hagood, J. S. (2007) Enhanced myofibroblastic differentiation and survival in Thy-1(-) lung fibroblasts. *Am. J. Respir. Cell Mol. Biol.* **36**, 226–235
44. Raghu, G., Rochwerg, B., Zhang, Y., Garcia, C. A., Azuma, A., Behr, J., Brozek, J. L., Collard, H. R., Cunningham, W., Homma, S., Johkoh, T., Martinez, F. J., Myers, J., Protzko, S. L., Richeldi, L., Rind, D., Selman, M., Theodore, A., Wells, A. U., Hoogsteden, H.,

and Schünemann, H. J.; American Thoracic Society; European Respiratory society; Japanese Respiratory Society; Latin American Thoracic Association. (2015) An official ATS/ERS/JRS/ALAT clinical practice guideline: treatment of idiopathic pulmonary fibrosis. An update of the 2011 clinical practice guideline. *Am. J. Respir. Crit. Care Med.* **192**, e3–e19; erratum: 644
45. Conte, E., Fruciano, M., Fagone, E., Gili, E., Caraci, F., Iemmolo, M., Crimi, N., and Vancheri, C. (2011) Inhibition of PI3K prevents the proliferation and differentiation of human lung fibroblasts into myofibroblasts: the role of class I P110 isoforms. *PLoS One* **6**, e24663
46. Tzouvelekis, A., Bonella, F., and Spagnolo, P. (2015) Update on therapeutic management of idiopathic pulmonary fibrosis. *Ther. Clin. Risk Manag.* **11**, 359–370
47. Selman, M., Pardo, A., Richeldi, L., and Cerri, S. (2011) Emerging drugs for idiopathic pulmonary fibrosis. *Expert Opin. Emerg. Drugs* **16**, 341–362
48. Behr, J., Bendstrup, E., Crestani, B., Günther, A., Olschewski, H., Sköld, C. M., Wells, A., Wuyts, W., Koschel, D., Kreuter, M., Wallaert, B., Lin, C. Y., Beck, J., and Albera, C. (2016) Safety and tolerability of acetylcysteine and pirfenidone combination therapy in idiopathic pulmonary fibrosis: a randomised, double-blind, placebo-controlled, phase 2 trial. *Lancet Respir. Med.* **4**, 445–453
49. Sakamoto, S., Muramatsu, Y., Satoh, K., Ishida, F., Kikuchi, N., Sano, G., Sugino, K., Isobe, K., Takai, Y., and Homma, S. (2015) Effectiveness of combined therapy with pirfenidone and inhaled N-acetylcysteine for advanced idiopathic pulmonary fibrosis: a case-control study. *Respirology* **20**, 445–452
50. Xia, H., Diebold, D., Nho, R., Perlman, D., Kleidon, J., Kahm, J., Avdulov, S., Peterson, M., Nerva, J., Bitterman, P., and Henke, C. (2008) Pathological integrin signaling enhances proliferation of primary lung fibroblasts from patients with idiopathic pulmonary fibrosis. *J. Exp. Med.* **205**, 1659–1672
51. Phan, S. H. (2008) Biology of fibroblasts and myofibroblasts. *Proc. Am. Thorac. Soc.* **5**, 334–337
52. Wang, J., Gambhir, A., Hangyás-Mihályné, G., Murray, D., Golebiewska, U., and McLaughlin, S. (2002) Lateral sequestration of phosphatidylinositol 4,5-bisphosphate by the basic effector domain of myristoylated alanine-rich C kinase substrate is due to nonspecific electrostatic interactions. *J. Biol. Chem.* **277**, 34401–34412
53. Moeller, A., Ask, K., Warburton, D., Gauldie, J., and Kolb, M. (2008) The bleomycin animal model: a useful tool to investigate treatment options for idiopathic pulmonary fibrosis? *Int. J. Biochem. Cell Biol.* **40**, 362–382
54. Myllärniemi, M., and Kaarteenaho, R. (2015) Pharmacological treatment of idiopathic pulmonary fibrosis - preclinical and clinical studies of pirfenidone, nintedanib, and N-acetylcysteine. *Eur. Clin. Respir. J.* **2**, eCollection 2015

Received for publication July 8, 2019.
Accepted for publication September 17, 2019.